Extreme ultraviolet emission from non-relativistic electrons penetrating a multilayer nanostructure

N.N. Nasonov [a,1], A.S. Kubankin [a], P.N. Zhukova [a], M. Goldstein [b], D.L. Williams [b], M.A. Piestrup [c], H. Park [c,*]

[a] *Laboratory of Radiation Physics, Belgorod State University, 14 Studencheskaya St., Belgorod 308007, Russia*
[b] *INTEL Corporation, 2200 Mission College Blvd, Santa Clara, CA 95052, USA*
[c] *Adelphi Technology Inc., 981-B Industrial Road, San Carlos, CA 94070, USA*

Abstract

The spectral and angular distributions from parametric X-radiation (PXR) from non-relativistic electrons penetrating a multilayer nanostructure are calculated while accounting for contributions of ordinary and diffracted transition radiation. The PXR emission mechanism is shown to be the dominant emission mechanism. The calculation also demonstrates the possibility of a tunable quasi-monochromatic extreme ultraviolet (EUV) source using only non-relativistic electrons whose efficiency can be large enough for practical applications.
© 2006 Elsevier B.V. All rights reserved.

1. Introduction

When a fast electron crosses a single interface between two media with different dielectric susceptibilities, electromagnetic radiation is emitted as predicted by Ginzburg and Frank [1]. Known as transition radiation (TR) and considered as a possible bright source of X-rays (in the case of relativistic emitting electrons), this emission mechanism has been studied both theoretically and experimentally [2–8].

Other forms of this radiation can occur depending upon the medium and periodicity of the radiator. For example, constructive interference of the waves emitted at periodically placed interfaces of the foils leads to the existence of intense narrow peaks of resonant transition radiation (RTR) [3,9–12]. Thin foils accurately spaced periodically in a vacuum have been used to produce RTR. For mechanical reasons, the period of such structure cannot be smaller than a few microns. However, another possible RTR radiator is a periodic multilayer nanostructure, commonly known as an X-ray mirror [13–20], which can have much smaller periods.

Crystals are periodic media and, hence, can also be emitters. PXR and diffraction transition radiation (DTR) emission mechanisms for relativistic electrons passing through crystals have been discussed in [21–28]. Diffracted transition radiation is TR emitted at the surface of the crystal and Bragg-scattered out by the crystalline atomic planes. PXR from non-relativistic electrons passing through crystals has been discussed in [29–34]. There has been some theoretical analysis of PXR and DTR from relativistic electrons passing through multilayers [13,18,35], but only

* Corresponding author. Tel.: +1 650 598 9800x17; fax: +1 650 598 9400.
E-mail addresses: nnn@bsu.edu.ru (N.N. Nasonov), hpark@adelphi-tech.com (H. Park).
[1] Tel.: +7 722 315726; fax: +7 722 301213.

one experiment [36,37]. This experiment demonstrated that an X-ray source using a multilayer can be larger than that using a crystal [34].

The possibility of using RTR from non-relativistic electrons moving through a multilayer nanostructure for quasi-monochromatic soft X-ray production was studied earlier [13,38–40]. In contrast to this, we consider the case of a multilayer for EUV generation by non-relativistic electrons using the PXR mechanism. In our opinion PXR offers a few advantages over RTR as the emission mechanism for producing EUV. Indeed, multilayers are usually supported by relatively thick substrates, which, in most cases, will absorb the emitted RTR whose emission cone is coaxial to the electron's direction. PXR is free from this disadvantage because the radiation is Bragg scattering out. The goal of our PXR analysis is to demonstrate the possibility of creating a very simple and intense source of EUV with a quasi-monochromatic and tunable spectrum for various applications. Previous work by some of us (Goldstein et al.) has investigated the use of modest-energy relativistic electrons for EUV emission from multilayers in free electron lasers and as stand-alone radiators [41].

Since the period of the multilayer can be comparable to the wavelength of emitted photons, we go beyond the scope of the Wentzel–Kramers–Brillouin approximation usually used in such analyses [3]. The more general approach based on the system of dynamic-diffraction equations [42] is used in our study. The influence of dynamic-diffraction effects on PXR properties is small in the case of non-relativistic electrons because of the great difference between dispersion laws for the primary virtual photon associated with the particle's Coulomb field and the secondary free photon of PXR field. Thus we will use a simple limit of the dynamic-diffraction theory known as kinematic scattering theory (or perturbation theory), which has been used with great success for the description of PXR from crystalline radiators.

In Section 2, we derive the general expressions for the emission of spectral and angular distributions. Contributions from TR, PXR and DTR are included. On the other hand, the influence of multiple scattering of emitting electrons, which brings into existence bremsstrahlung and destroys the coherency in PXR and DTR, is not taken into account in this paper, which is devoted to determining the maximum possible emission. Characteristics of the photon flux produced by non-relativistic electrons penetrating the multilayer nanostructure are studied in Section 3 on the basis of formulae obtained in Section 2. Our conclusions and final remarks are given in Section 4. The system of units $c = 1$ is used in the paper.

2. Spectral–angular distribution

Let us consider an emission from electrons penetrating into a multilayer nanostructure as it is shown in Fig. 1. We will first determine the periodically changing dielectric susceptibility of the multilayer $\chi_0(\omega, x) = \chi_0(\omega) +$
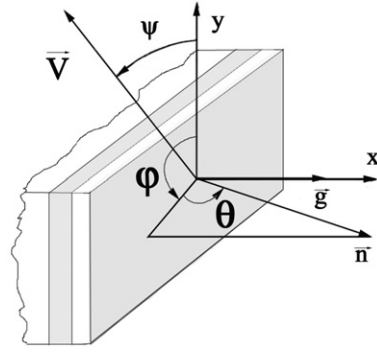

Fig. 1. The geometry of the emission process. $\vec{g}$ is the reciprocal lattice vector, $\vec{V}$ is the velocity of an emitting electron, $\vec{n}$ is the unit vector to the direction of emitted photon propagation.

$\sum_{\vec{g} \neq 0} \chi_g(\omega) e^{igx}$. For the case of a one-dimensional structure consisting of alternative layers with thicknesses a and b and susceptibilities $\chi_a(\omega)$ and $\chi_b(\omega)$, respectively, the quantities $\chi_0(\omega)$ and $\chi_g(\omega)$ are determined by the expressions

$$\chi_0(\omega) = \frac{a}{T}\chi_a(\omega) + \frac{b}{T}\chi_b(\omega),$$

$$\chi_g(\omega) = \frac{1 - e^{iga}}{igT}(\chi_a - \chi_b), \tag{1}$$

where $T = a + b$ is the period of multilayer structure, $g = (2\pi/T)n$, $n = 0, \pm 1, \pm 2, \ldots$

The solutions to Maxwell equations for electromagnetic fields excited by a fast electron moving through the layered structure may be obtained using previous treatments [8,9,11,16,18,20]. However, we cannot use the final results of these works since they have been obtained for normal-incidence electrons onto the surface of the target. Also we wish to vary the incidence angle in order to change the energy of emitted photons. For the general case, the exact solutions are rather complicated and inconvenient for physical analysis. On the other hand, the analysis [20] developed using the Kronig–Penney model has shown that in X-ray range ($|\chi| \ll 1$) the exact solution is equivalent to the two-wave approximation of dynamic diffraction theory [42], which is very convenient for describing the emission process. Within the frame of the dynamic-diffraction theory the Fourier-transform of electric field $\vec{E}_{\omega\vec{k}} = (2\pi)^{-4} \int dt\, d^3r \vec{E}(\vec{r}, t) e^{-i\vec{k}\vec{r} + i\omega t}$ is determined by the equations

$$(k^2 - \omega^2(1 + \chi_0))\vec{E}_{\omega k} - \vec{k}(\vec{k} \cdot \vec{E}_{\omega k}) - \omega^2 \sum_{g \neq 0} \chi_{-\vec{g}}\vec{E}_{\omega\vec{k}+\vec{g}}$$

$$= \frac{i\omega e}{2\pi^2}\vec{V}\delta(\omega - \vec{k}\vec{V}),$$

$$((\vec{k}+\vec{g})^2 - \omega^2(1 + \chi_0))\vec{E}_{\omega\vec{k}+\vec{g}} - (\vec{k}+\vec{g})\left((\vec{k}+\vec{g}) \cdot \vec{E}_{\omega\vec{k}+\vec{g}}\right)$$

$$= \omega^2\chi_g\vec{E}_{\omega\vec{k}} + \omega^2 \sum_{g' \neq 0 \neq -g} \chi_{-g'}\vec{E}_{\omega\vec{k}+\vec{g}+\vec{g}'}, \tag{2}$$

where $\vec{V}$ is the emitting electron velocity.

Eq. (2) was used earlier to determine the PXR and DTR generation by electrons crossing multilayers [35]. The two-wave approximation of dynamic-diffraction theory can be used to study the case of relativistic electrons with their Coulomb field was nearly transverse and $k^2 \approx \omega^2$, so that the dynamic-diffraction effects can be substantial. On the other hand, for non-relativistic emitting electrons, $k^2 \sim \omega^2/V^2 \gg \omega^2$, and the influence of dynamic-diffraction effects on PXR properties is small. As this takes place, Eq. (2) can be reduced to very simple equations of the kinematic theory of PXR:

$$(k^2 - \omega^2(1+\chi_0))\vec{E}_{\omega k} - \vec{k}(\vec{k}\cdot\vec{E}_{\omega k}) = \frac{i\omega e}{2\pi^2}\vec{V}\delta(\omega - \vec{k}\vec{V}), \quad (3a)$$

$$((\vec{k}+\vec{g})^2 - \omega^2(1+\chi_0))\vec{E}_{\omega\vec{k}+\vec{g}}$$
$$- (\vec{k}+\vec{g})\Big((\vec{k}+\vec{g})\cdot\vec{E}_{\omega\vec{k}+\vec{g}}\Big) = \omega^2\chi_g\vec{E}_{\omega\vec{k}}. \quad (3b)$$

Obviously, Eqs. (3a) and (3b) give an adequate description of the process being considered with the proviso that the reflection coefficient from a single bi-layer is small. This is true far from the conditions of total external reflection, i.e. the grazing angle of the photon momentum vector relative to the plane of layers must exceed the corresponding critical angle $\sqrt{|\chi_0|}$. When solving Eq. (3a), one should take into account two facts. First, the distinctive property of the emission from non-relativistic electrons consists in the substantial contribution of the longitudinal component of this electron's Coulomb field to the formation of the emission yield. Thus, the vector $\vec{E}_{\omega\vec{k}}$ must be expanded into three polarization vectors:

$$\vec{E}_{\omega\vec{k}} = \sum_{\lambda=1}^{2}\vec{e}_{\lambda 0}\vec{E}_{\lambda 0}, \quad (4)$$

where $\vec{e}_{10} = \frac{\vec{k}_\parallel \times \vec{e}_x}{k_\parallel}$, $\vec{e}_{20} = \frac{\vec{k}_\parallel k_x \times \vec{e}_x k_\parallel^2}{k_\parallel \cdot k}$ and $\vec{e}_{30} = \frac{\vec{k}}{k}$.

For the case of ultra-relativistic particles, only the terms $\vec{e}_{10}$ and $\vec{e}_{20}$ would be needed.

The second fact, which is unique to the process of EUV generation, is the strong photoabsorption. We will assume that the thickness of the multilayer nanostructure is larger than the photoabsorption length and, hence, the multilayer may be considered as a semi-infinite one.

Using Eqs. (3a) and (4), the formula $\vec{H}_{\omega\vec{k}} = \frac{1}{\omega}\vec{k}x\vec{E}_{\omega\vec{k}}$, and the ordinary boundary conditions for electromagnetic fields at the surface of the multilayer, one can obtain the following formulae describing the electromagnetic field $\vec{E}_{\omega\vec{k}} \equiv \vec{E}_{\omega\vec{k}}^{(m)}$ inside the multilayer:

$$E_{\lambda 0}^{(m)} = a_{\lambda 0}^{(m)}\delta\Big(k_x + \sqrt{\omega^2\varepsilon - k_\parallel^2}\Big) + \frac{i\omega e}{2\pi^2|V_x|}\frac{\vec{e}_{\lambda 0}\vec{V}}{k_x^2 - \omega^2\varepsilon + k_\parallel^2}\delta(k_x - k_\perp),$$

$$\lambda = 1, 2,$$

$$E_{30}^{(m)} = -\frac{ie}{2\pi^2|V_x|}\frac{1}{k\varepsilon}\delta(k_x - k_\perp),$$

$$a_{10}^{(m)} = \frac{i\omega e}{2\pi^2|V_x|}\cdot\vec{e}_{10}\vec{V}\frac{\sqrt{\omega^2 - k_\parallel^2} - k_\perp}{\sqrt{\omega^2 - k_\parallel^2} + \sqrt{\omega^2\varepsilon - k_\parallel^2}}$$
$$\times\left(\frac{1}{k_\perp^2 - \omega^2 + k_\parallel^2} - \frac{1}{k_\perp^2 - \omega^2\varepsilon + k_\parallel^2}\right)$$

$$a_{20}^{(m)} = -\frac{i\omega e}{2\pi^2|V_x|}\cdot\frac{\sqrt{\varepsilon}}{\omega k_\parallel}\left[\Big(\sqrt{\omega^2 - k_\parallel^2}\cdot\vec{k}_\parallel\vec{V}_\parallel + k_\parallel^2 V_x\Big)\right.$$
$$\times\frac{\sqrt{\omega^2 - k_\parallel^2} - k_\perp}{\varepsilon\sqrt{\omega^2 - k_\parallel^2} + \sqrt{\omega^2\varepsilon - k_\parallel^2}}\left(\frac{1}{k_\perp^2 - \omega^2 + k_\parallel^2} - \frac{1}{k_\perp^2 - \omega^2\varepsilon + k_\parallel^2}\right)$$
$$\left.-\frac{\chi_0}{\varepsilon}\frac{\omega}{\varepsilon\sqrt{\omega^2 - k_\parallel^2} + \sqrt{\omega^2\varepsilon - k_\parallel^2}}\cdot\frac{k_\parallel^2}{k_\perp^2 - \omega^2\varepsilon + k_\parallel^2}\right], \quad (5)$$

where $k_\perp = \frac{1}{V_x}(\omega - \vec{k}_\parallel\vec{V}_\parallel)$, $\varepsilon(\omega) = 1 + \chi_0(\omega)$.

The result Eq. (5) will be used in further studies of diffracted fields. On the other hand, the transverse components of the electric field in a vacuum outside the target $\vec{E}_{\omega\vec{k}} \equiv \vec{E}_{\omega\vec{k}}^{(V)}$:

$$E_{\lambda 0}^{(V)} = a_{\lambda 0}^{(V)}\delta\Big(k_x - \sqrt{\omega^2 - k_\parallel^2}\Big)$$
$$+ \frac{i\omega e}{2\pi^2|V_x|}\frac{\vec{e}_{\lambda 0}\vec{V}}{k_x^2 - \omega^2 + k_\parallel^2}\delta(k_x - k_\perp),$$
$$\lambda = 1, 2, \quad (6)$$

where

$$a_{10}^{(V)} = \frac{i\omega e}{2\pi^2|V_x|}\cdot\vec{e}_1\vec{V}\frac{\sqrt{\omega^2\varepsilon - k_\parallel^2} + k_\perp}{\sqrt{\omega^2\varepsilon - k_\parallel^2} + \sqrt{\omega^2 - k_\parallel^2}}$$
$$\times\left(\frac{1}{k_\perp^2 - \omega^2 + k_\parallel^2} - \frac{1}{k_\perp^2 - \omega^2\varepsilon + k_\parallel^2}\right)$$

$$a_{20}^{(V)} = -\frac{i\omega e}{2\pi^2|V_x|}\cdot\frac{1}{\omega k_\parallel}\left[\Big(\sqrt{\omega^2\varepsilon - k_\parallel^2}\cdot\vec{k}_\parallel\vec{V}_\parallel - k_\parallel^2 V_x\Big)\right.$$
$$\times\frac{\sqrt{\omega^2\varepsilon - k_\parallel^2} + k_\perp}{\sqrt{\omega^2\varepsilon - k_\parallel^2} + \varepsilon\sqrt{\omega^2 - k_\parallel^2}}\left(\frac{1}{k_\perp^2 - \omega^2 + k_\parallel^2} - \frac{1}{k_\perp^2 - \omega^2\varepsilon + k_\parallel^2}\right)$$
$$\left.-\chi_0\frac{\omega}{\sqrt{\omega^2\varepsilon - k_\parallel^2} + \varepsilon\sqrt{\omega^2 - k_\parallel^2}}\cdot\frac{k_\parallel^2}{k_\perp^2 - \omega^2 + k_\parallel^2}\right].$$

Eq. (6) describes the transition radiation field contributing to total emission yield. To find this contribution one should determine the emission field in the wave zone:

$$E_\lambda^{\mathrm{TR}} = \int d^3k\,e^{i\vec{k}\vec{n}\vec{r}}a_{\lambda 0}^{(V)}\delta\Big(k_x - \sqrt{\omega^2 - k_\parallel^2}\Big), \quad (7)$$

where $\vec{n}$ is the unit vector to the direction of emitted photon propagation. The result of integration in Eq. (7) obtained by the stationary phase method has the form

$$E_\lambda^{\text{TR}} = A_\lambda^{\text{TR}} \frac{e^{i\omega r}}{r}, \quad A_\lambda^{\text{TR}} = -2\pi i \omega n_x a_{\lambda 0}^{(V)}|_{\vec{k}_\parallel = \omega \vec{n}_\parallel}, \tag{8}$$

where $\vec{n}_\parallel = \vec{n}_y + \vec{n}_z$. Spectral–angular distribution of emitted transition radiation quanta following from Eq. (8) can be presented as

$$\omega \frac{dN^{\text{TR}}}{d\omega d\Omega} = \sum_{\lambda=1}^{2} \omega \frac{dN_\lambda^{\text{TR}}}{d\omega d\Omega},$$

$$\omega \frac{dN_1^{\text{TR}}}{d\omega d\Omega} = \frac{e^2}{\pi^2} \frac{|\chi_0|^2}{|n_x + \sqrt{n_n^2 + \chi_0}|^2} \frac{1}{n_\parallel^2}$$

$$\cdot \frac{n_x^2 ((\vec{n}_\parallel \times \vec{e}_x) \cdot \vec{V})^2 V_x^4}{|1 - \vec{n}_\parallel \vec{V}_\parallel - \sqrt{n_x^2 + \chi_0} V_x|^2 [(1 - \vec{n}_\parallel \vec{V}_\parallel)^2 - n_x^2 V_x^2]^2}, \tag{9}$$

$$\omega \frac{dN_2^{\text{TR}}}{d\omega d\Omega} = \frac{e^2}{\pi^2} \frac{|\chi_0|^2}{|\varepsilon n_x + \sqrt{n_n^2 + \chi_0}|^2} \frac{1}{n_\parallel^2}$$

$$\cdot \frac{n_x^2 |n_\parallel^2 (1 - \vec{n}_\parallel \vec{V}_\parallel - \sqrt{n_x^2 + \chi_0} V_x) + (\sqrt{n_x^2 + \chi_0} \vec{n}_\parallel \vec{V}_\parallel - n_\parallel^2 V_x) V_x|^2 V_x^2}{|1 - \vec{n}_\parallel \vec{V}_\parallel - \sqrt{n_x^2 + \chi_0} V_x|^2 [(1 - \vec{n}_\parallel \vec{V}_\parallel)^2 - n_x^2 V_x^2]^2}.$$

Eq. (9) describes the part of total emission that should be considered as a broadband background only. The contribution of interest to us is formed in the process of the field Eq. (5) diffraction by periodic heterogeneities of multilayer's electron density. The diffracted field

$$\vec{E}_{\omega \vec{k} + \vec{g}} = \sum_{\lambda=1}^{3} \vec{e}_{\lambda g} E_{\lambda g}, \tag{10}$$

where $\vec{e}_{1g} = \vec{e}_{10}$, $\vec{e}_{2g} = \frac{\vec{k}_\parallel k_{gx} - \vec{e}_x k_\parallel^2}{k_\parallel}$, and $\vec{e}_{3g} = \frac{\vec{k}_g}{k_g}$. $\vec{k}_g = \vec{k} + \vec{e}_x g$, is determined by the solution of Eq. (3b), which should be found separately inside and outside the multilayer nanostructure.

The general solution of Eq. (3b) describing transverse components of the diffracted field inside the target $\vec{E}_{\omega \vec{k} + \vec{g}}^{(m)}$ has the form

$$E_{\lambda g}^{(m)} = a_{\lambda g}^{(m)} \delta \left(k_{gx} + \sqrt{\omega^2 \varepsilon - k_\parallel^2} \right) + \frac{\omega^2 \chi_g \vec{e}_{\lambda g} \vec{E}_{\omega \vec{k}}^{(m)}}{k_{gx}^2 - \omega^2 \varepsilon + k_\parallel^2},$$

$$\lambda = 1, 2. \tag{11}$$

The quantity $\vec{E}_{\omega \vec{k}}^{(m)}$ in Eq. (11) is determined by formulae (5). On the basis of Eqs. (3b), (10) and (11) and the general formula for the diffracted field in a vacuum outside the target:

$$E_{\lambda g}^{(V)} = a_{\lambda g}^{(V)} \delta \left(k_{gx} - \sqrt{\omega^2 \varepsilon - k_\parallel^2} \right), \quad \lambda = 1, 2, \tag{12}$$

one can determine the unknown coefficients $a_{\lambda g}^{(V)}$ by means of the necessary boundary conditions. The final expressions for $a_{\lambda g}^{(V)}$ may be presented in the form

$$a_{1g}^{(V)} = \frac{\omega^2 \chi_g}{\sqrt{\omega^2 \varepsilon - k_\parallel^2} + \sqrt{\omega^2 - k_\parallel^2}} \cdot \left[\frac{1}{g - 2\sqrt{\omega^2 \varepsilon - k_\parallel^2}} a_{10}^{(m)} \right.$$

$$\left. + \frac{1}{g + k_\perp - \sqrt{\omega^2 \varepsilon - k_\parallel^2}} \cdot \frac{i\omega e}{2\pi^2 |V_x|} \frac{\vec{e}_{10} \vec{V}}{k_\perp^2 - \omega^2 \varepsilon + k_\parallel^2} \right],$$

$$a_{2g}^{(V)} = \frac{\omega \chi_g}{\sqrt{\omega^2 \varepsilon - k_\parallel^2} + \varepsilon \sqrt{\omega^2 - k_\parallel^2}}$$

$$\cdot \left[\frac{1}{g - 2\sqrt{\omega^2 \varepsilon - k_\parallel^2}} \frac{2k_\parallel^2 - \omega^2 \varepsilon}{\omega \sqrt{\varepsilon}} a_{20}^{(m)} \right.$$

$$+ \frac{1}{g + k_\perp - \sqrt{\omega^2 \varepsilon - k_\parallel^2}} \cdot \frac{i\omega e}{2\pi^2 |V_x|} \frac{1}{k_\parallel}$$

$$\left. \times \left(\frac{\sqrt{\omega^2 \varepsilon - k_\parallel^2} \vec{k}_\parallel \vec{V}_\parallel - k_\parallel^2 V_x}{k_\perp^2 - \omega^2 \varepsilon + k_\parallel^2} + \frac{k_\parallel^2}{\omega \varepsilon} \frac{1}{k_\perp \sqrt{\omega^2 \varepsilon + k_\parallel^2}} \right) \right]. \tag{13}$$

Both PXR and DTR contribute to the diffracted radiation field described by formulae (12) and (13). In order to determine the diffracted radiation amplitude A_λ^{DR} one should calculate Fourier integral $E_\lambda^{\text{DR}} = \int d^3 k_g e^{i\vec{k}_g \vec{n} r} a_{\lambda g}^{(V)} \delta \left(k_{g\lambda} - \sqrt{\omega^2 - k_\parallel^2} \right)$ as was done with Eq. (7). Obviously, the result of integration coincides with Eq. (8):

$$A_\lambda^{\text{DR}} = -2\pi i \omega n_x a_{\lambda g}^{(V)}|_{\vec{k}_\parallel = \omega \vec{n}_\parallel}. \tag{14}$$

Since the formula describing the spectral–angular distribution of diffracted radiation

$$\omega \frac{dN^{\text{DR}}}{d\omega d\Omega} = \sum_{\lambda=1}^{2} |A_\lambda^{\text{DR}}|^2 \tag{15}$$

is very complicated in the general case, the special case of EUV emission will be analyzed in the next section.

3. Properties of the diffracted radiation

Characteristics of the diffracted radiation are completely determined by the results Eqs. (5), (13)–(15). Embarking on a study of these characteristics, we emphasize that the π-polarization ($\lambda = 2$) makes the main contribution to total emission yield in the case of non-relativistic emitting electrons ($V \ll 1$) under consideration. For example, in the case $V \ll 1$, formulae (9) describing the background determined by transition radiation are reduced to a simple one:

$$\omega \frac{dN^{\text{TR}}}{d\omega d\Omega} = \omega \frac{dN_2^{\text{TR}}}{d\omega d\Omega}$$

$$\approx \frac{e^2}{\pi^2} \frac{|\chi_0|^2}{|\varepsilon n_x + \sqrt{n_x^2 + \chi_0}|^2}$$

$$\cdot \frac{n_x^2 n_\parallel^2 V_x^2}{(1 - \vec{n}_\parallel \vec{V}_\parallel - n_x V_x)^2 [1 - \vec{n}_\parallel \vec{V}_\parallel - n_x V_x^2]^2}. \tag{16}$$

In contrast with broadband spectrum Eq. (16), the distribution of diffracted radiation given by Eqs. (13)–(15) is typical of quasi-monochromatic spectra. In accordance with Eq. (13), there are two peaks caused by the different emission processes. In order to study these peaks, let us consider the expression for total emission amplitude following from Eqs. (5), (13) and (14) in the case of non-relativistic emitting electrons in question:

$$
\begin{aligned}
A^{DR} &\approx A_2^{DR} \\
&\approx \frac{e}{\pi \varepsilon} \frac{\chi_g}{\varepsilon n_x + \sqrt{n_x^2 + \chi_0}} \cdot \frac{n_x n_\parallel |V_x|}{1 - \vec{n}_\parallel \vec{V} + \sqrt{n_x^2 + \chi_0} V_x} \\
&\times \left[\frac{\chi_0}{\varepsilon n_x + \sqrt{n_x^2 + \chi_0}} \cdot \frac{n_\parallel^2 - n_x^2 - \chi_0}{1 - \vec{n}_\parallel \vec{V}_\parallel - \sqrt{n_x^2 + \chi_0}} \right. \\
&\left. \cdot \frac{1}{\frac{g}{\omega} - 2\sqrt{n_x^2 + \chi_0}} + \frac{1}{\frac{gV_x}{\omega} + 1 - \vec{n}_\parallel \vec{V}_\parallel - \sqrt{n_x^2 + \chi_0} V_x} \right].
\end{aligned}
\tag{17}
$$

The obtained result shows that the first peak in the spectrum of diffracted radiation is determined by the condition

$$
\omega = \frac{g}{2\mathrm{Re}(\sqrt{n_x^2 + \chi_0})} \approx \frac{g}{2n_x} = \omega^{DTR}.
\tag{18}
$$

The resonance frequency $g/2n_x$ is analogous to the Bragg frequency used in X-ray diffraction theory. The corresponding term in the amplitude Eq. (17) describes peak emission occurring due to the diffraction of free photons of the TR field propagating in the target. The formula (13) shows that this term is proportional to the coefficient $a_{20}^{(m)}$, which describes TR in the general formula (5). Thus, the peak emission is from DTR.

In accordance with Eq. (17), the second peak in the spectrum of diffracted radiation is located in the velocity of the frequency

$$
\omega = \frac{g|V_x|}{1 - \vec{n}_\parallel \vec{V}_\parallel - \mathrm{Re}(\sqrt{n_x^2 + \chi_0})V_x} \approx \frac{|\vec{g}\vec{V}|}{1 - \vec{n}\vec{V}} = \omega^{PXR}.
\tag{19}
$$

The resonance frequency given by Eq. (19) is very close to that in PXR theory. This peak occurs due to the diffraction of virtual photons associated with a fast electron's Coulomb field. The δ-functions on the formula (5) describing the primary electromagnetic field scattered by periodic heterogeneities of the multilayer, showing that the peak under study is formed by the diffraction of virtual photons with wave vectors $k \approx \omega/V$ in contrast with the previous peak formed by the diffraction of real photons with wave vectors $k \approx \omega\sqrt{\varepsilon}$.

It should be noted that the difference between resonance frequencies Eqs. (18) and (19) is conditioned by the non-relativistic character of the emitting electrons. Indeed, in the case of relativistic emitting particles, the primary electromagnetic field, including both virtual photons of Coulomb field and real photons of TR, propagate along the velocity direction of the emitting particle. The intensity of this field is concentrated in the interior of a narrow angular

cone of the order of $\gamma^{-1} \ll 1$ (γ is the Lorentz factor of relativistic electron). As a consequence, the diffracted secondary electromagnetic field propagates in the mirror direction (this direction is determined by the condition $\varphi = 0$, $\theta = \psi$; angles φ, θ and ψ are presented in Fig. 1), so that the equality

$$
\omega_{DTR} = \frac{g}{2\sin(\psi)} = \frac{g\sin(\psi)}{1 - \cos(2\psi)} = \omega^{PXR}
\tag{20}
$$

is valid.

Let us consider PXR spectral–angular distribution. Using the results Eqs. (15) and (17) and introducing the angular variables φ, θ and ψ by formulae

$$
\begin{aligned}
&V_x = -V\sin(\psi), \; V_y = V\cos(\psi), \; V_z = 0, \\
&n_x = \sin(\theta), \; n_y = \cos(\theta)\cdot\cos(\varphi), \; \text{and} \; n_z = \cos(\theta)\cdot\sin(\varphi),
\end{aligned}
\tag{21}
$$

one obtains the following formula:

$$
\begin{aligned}
\omega &\frac{dN^{PXR}}{d\omega d\Omega} \\
&= \frac{e^2 V^2}{\pi^4} \sin^2\left(\pi\frac{a}{T}\right) \frac{(\chi_a' - \chi_b')^2 + (\chi_a'' - \chi_b'')^2}{(1 + \chi_0')^2 + (\chi_0'')^2} \\
&\cdot \frac{\sin^2(\theta)\cos^2(\theta)}{(f' + (1+\chi_0')^2\sin(\theta))^2 + (f'' + \chi_0''\sin(\theta))^2} \\
&\cdot \frac{\sin^2(\psi)}{(1 - V\cos(\psi)\cos(\theta)\cos(\varphi) - Vf'\sin(\psi))^2 + (Vf''\sin(\psi))^2} \\
&\cdot \frac{1}{\left(\frac{gV\sin(\psi)}{\omega} - 1 + V\cos(\psi)\cos(\theta)\cos(\varphi) - Vf'\sin(\psi)\right)^2 + (Vf''\sin(\psi))^2},
\end{aligned}
\tag{22}
$$

where the quantities f' and f'' are determined by

$$
f' = \frac{1}{\sqrt{2}}\sqrt{\sqrt{(\sin^2(\theta) + \chi_0')^2 + (\chi_0'')^2} + \sin^2(\theta) + \chi_0'},
$$

$$
f'' = \frac{1}{\sqrt{2}}\sqrt{\sqrt{(\sin^2(\theta) + \chi_0')^2 + (\chi_0'')^2} - \sin^2(\theta) - \chi_0'}.
\tag{23}
$$

It is of first importance that the distribution Eq. (22) describes the predominant contribution to total emission yield in the vicinity of the frequency $\omega = \omega^{PXR}$. Comparison of Eqs. (16) and (22) shows that the values of TR and PXR contributions to total emission yield are of the same order outside the vicinity of ω^{PXR}. As for the DTR contribution, it can dominate in the vicinity of $\omega = \omega^{DTR}$, but this contribution is small compared with the PXR one outside this vicinity because of the additional factor $|\chi_0|^2 \ll 1$ in DTR cross-section (this factor corresponds to the transformation of virtual photons of the Coulomb field to real photons of TR).

Let us consider in greater detail the distribution Eq. (22). One of the most important properties of PXR from non-relativistic electrons following from Eq. (22) consists in the strong dependence of the PXR spectral peak position on the value of the emitting electron velocity V and the orientation angle ψ. On the other hand, such dependence on

the observation angles θ and φ is weak because of this small value of the velocity V. Outlined properties allows us to vary the energy of emitted photons by changing the angle ψ with no attendant change of the emission angular distribution as in the case of PXR from relativistic electrons.

Spectral width of the PXR peak

$$\Delta\omega \approx gf''V^2\sin^2(\psi) \approx \frac{g\chi_0''V^2\sin^2(\psi)}{2\sqrt{\sin^2(\theta)+\chi_0'}}, \qquad (24)$$

strongly depends on ψ, but the maximum of the emission density,

$$\left(\omega\frac{dN^{PXR}}{d\omega\,d\Omega}\right)_{max} \approx \frac{e^2}{\pi^4}\sin^2\left(\pi\frac{a}{T}\right)\left(\frac{\chi_a'-\chi_b'}{1+\chi_0'}\right)^2$$
$$\cdot\frac{\sin^2(\theta)\cos^2(\theta)}{(f'+(1+\chi_0')^2\sin(\theta))^2}\cdot\frac{1}{(f'')^2}\bigg|_{\omega\approx gV\sin(\varphi)} \qquad (25)$$

depends on ψ and V through the mediation of the dispersion of dielectric susceptibilities $\chi_a(gV\sin(\psi))$ and $\chi_b(gV\sin(\psi))$ only.

Note, the estimation Eq. (24) presents the natural PXR spectral width only. Additional growth of the spectral width is caused by both the finite number of periods in the layered structure and the influence of multiple scattering of the electrons. The first effect is responsible for the width $\Delta\omega_1 \approx gV\sin(\psi)/N_0$, where N_0 is the number of periods. The minimum value of $\Delta\omega_1$ is determined by the maximum possible N_0 bounded by a photoabsorption

$$\Delta\omega_{1min} \approx 4\pi\Delta\omega, \qquad (26)$$

where $\Delta\omega$ is given by Eq. (24). Obviously, $\Delta\omega_1 \gg \Delta\omega$.

A strong influence of the multiple scattering on PXR spectral width immediately follows from Eq. (19). The width determined by multiple scattering is described by the formula:

$$\Delta\omega_2 \approx gV\cos(\Psi)\sqrt{\overline{\Delta^2\Psi}}, \qquad (27)$$

where $\overline{\Delta^2\Psi}$ is the averaged square of the angle of multiple scattering achievable at the distance $l \approx \sin(\theta)/gV\sin^2(\Psi)\chi''$ on which the electron emits photons capable of escaping the target. Using the formula for $\overline{\Delta^2\Psi}$:

$$\Delta^2\Psi = \frac{16\pi Z(Z+1)e^4n_0}{m^2E^2}\frac{(E+1)^2}{(E+2)^2}\ln(183Z^{-\frac{1}{3}})l, \qquad (28)$$

where $E = T_0/m$, Z is the atomic number, n_0 is the density of atoms, T_0 is the kinetic energy of an emitting electron, one can obtain the following estimation for the value of $\Delta\omega_2$:

$$\Delta\omega_2 \approx \frac{4e^2}{mE}\frac{E+1}{E+2}[(\pi/\chi_0'')Z(Z+1)\ln(183Z^{-1/3})n_0gV$$
$$\times\sin(\theta)]^{1/2}\cot(\Psi). \qquad (29)$$

The strong difference between the dependencies $\Delta\omega_1(\chi_0'')$ and $\Delta\omega_2(\chi_0'')$ is noteworthy. Obviously, the growth of photoabsorption increases PXR spectral width caused by the finite number of periods in nanostructure. On the other hand, an influence of the multiple scattering on PXR decreases with increasing χ_0''. Both of the outlined properties are explained by the reduction in the effective path of an emitting electron in the target.

The comparison of $\Delta\omega_1$ and $\Delta\omega_2$ shows that the multiple scattering dominates in the formation of the spectral width of PXR from electrons with energies of the order of 100 keV emitting photons in the frequency range $\omega \approx 100$ eV, where the imaginary part of the dielectric susceptibility has the value of the order of 0.001–0.01.

Let us estimate PXR spectral width in circumstances where a 100 keV electron beam moves through a thick Si–Nb multilayered nanostructure with the period T of the order of 100 Å, $a/T = 0.6$, a is the thickness of Si layer. The energy of an emitted photon is assumed to be close to 90 eV. Using the formulas (19) and (29) one can show that the relative PXR spectral width $\Delta\omega_2/\omega$ ranges up to 0.5–1 versus the values of the angles Ψ and ϑ.

In such a manner multiple scattering of emitting non-relativistic electrons plays an important role in the formation of PXR spectrum, which is why one should constrain the thickness of the radiator in order to obtain a quasi-monochromatic photon beam (in this case the PXR spectral width is determined by the number of periods in nanostructure). In any event, the influence of multiple scattering on the properties of PXR from non-relativistic electrons must be considered theoretically in detail.

As might be expected from an emission of non-relativistic electrons, PXR is characterized by smooth angular dependence. This is a substantial disadvantage of the EUV source being discussed. On the other hand, it is precisely this property that allows us to change the average energy of the collimated photon flux without large variations of the PXR intensity by rotating the multilayer relative to the axis of the electron beam and the photon collimator.

The possibility of producing a quasi-monochromatic, tunable EUV source is of prime interest to our study [41]. As a rule, susceptibilities $\chi_{a,b}(\omega)$ are fast varying functions of ω in this frequency range. Because of this, the correct choice of materials for creating neighboring layers in the multilayer nanostructure is of first importance. Since PXR intensity is proportional to $|\chi_a - \chi_b|^2$, experimental conditions, where susceptibilities χ_a and χ_b have different signs, show up as most convenient for EUV generation. To realize such conditions it is necessary to choose the material for one of two neighboring layers in such a way that the characteristic energy of PXR photons ω^{PXR}, determined by Eq. (19), is placed near to photoabsorption edge of this material. As this takes place, the susceptibility (e.g. χ_a) can be positive. In contrast to this, the dielectric susceptibility of the other layer χ_b must be negative in the vicinity of ω^{PXR}.

A special code has been developed to select the optimum pair of neighboring layers for EUV production at desired energies. For instance, it has been shown that Si–Nb layer pair is best suited for EUV production in the frequency range close to 100 eV. It is important to keep in mind that many parameters, such as the period of nanostructure, the orientation angle ψ, and the observation angles, θ and φ (for the case of large-enough values of the velocity of emitting electrons) must be chosen close to their optimum values in order to realize advantages of the approach being discussed. The above code permits us to solve this task.

Let us determine the maximum emission of a EUV source using numerical calculations of the PXR spectral characteristics developed in this paper. We have calculated the spectrum of strongly collimated PXR from 100-keV electrons penetrating a Si–Nb multilayer using Eq. (22) for fixed observation angles θ, φ and different values of the orientation angle ψ. The curves presented in Fig. 2 were calculated by using both the real and imaginary parts of Si and Nb dielectric susceptibilities, which were determined experimentally [43]. The period of multilayer was chosen in such a way that the characteristic frequency ω^{PXR} was far from Si L-edge. In contrast to this, the curves presented

in Fig. 3 describe the PXR spectrum for the special case where ω^{PXR} is brought into the vicinity of Si L-edge. When the last result is compared with the previous one, it is apparent that the PXR spectral density can substantially grow in amplitude in the vicinity of a photoabsorption edge, but the yield is strongly suppressed if the photon energy ω exceeds the critical energy of a photoabsorption edge.

Upon integrating Eq. (22) over observation angles, we obtain the spectrum of total PXR yield. The curves presented in Fig. 4 allow us to estimate PXR intensity as 10^{-6} photon/electron. This value is typical of PXR from relativistic electrons. Thus, the intensity of the emission mechanism under study may be high enough for some applications. This conclusion does not take into account the broadband bremsstrahlung background, which leads to high requirements for both the angular aperture and the photon-energy resolution of the detector used for detecting PXR from non-relativistic electrons in a crystalline target [34]. Such requirements are strongly reduced for PXR from a multilayered nanostructure because of the higher emission intensity when compared to that of a crystal [35] (the emission yield from 0.35 μm multilayer WB$_4$C nanostructure obtained in experiment [36] was higher than that from 100-μm crystalline Si substrate). The effect occurs because a larger number of multilayer's electrons make a coherent contribution to the formation of X-ray yield (for an extended discussion see [35]).

As shown in Fig. 4, there is a strong dependence of the PXR yield on the average observation angle $\langle\theta\rangle$. This is determined by the fact that the velocity V for the case of 100 keV emitting electrons has a large-enough value and results in a strong dependence of the characteristic PXR energy ω^{PXR} on the observation angle θ. Among other things, the dependence $\omega^{\mathrm{PXR}}(\theta)$, presented in Fig. 5 and calculated by Eq. (19) using the same parameters as those used in Fig. 4, exceeds the critical energy of Si L-edge for small values of θ. The PXR yield is strongly suppressed due to photoabsorption in accordance with curves presented in Fig. 4.
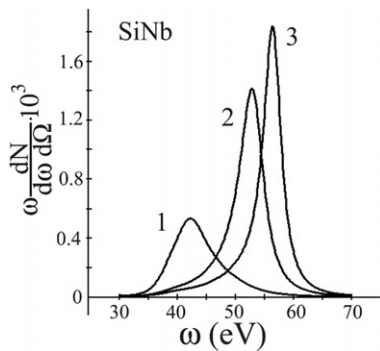

Fig. 2. The spectrum of strongly collimated PXR from 100 keV electrons penetrating multilayer nanostructure. Presented curves have been calculated in the case $\Theta = \pi/4$, $\varphi = 0$, $T = 100$ Å, $a/T = 0.6$, $\Psi = \pi/6$ (curve 1), $\Psi = \pi/4$ (curve 2) and $\Psi = \pi/3$ (curve 3).
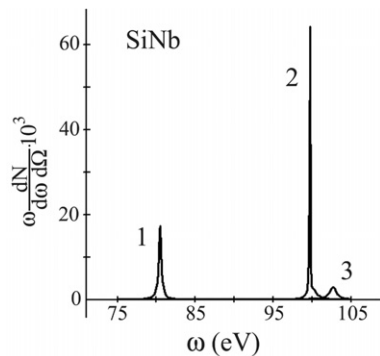

Fig. 3. The spectrum of strongly collimated PXR in the special case that ω^{PXR} is brought into the vicinity of Si L-edge. Presented curves have been calculated in the case $\Theta = 0.8$, $\varphi = 0$, $T = 45$ Å, $a/T = 0.6$, $\Psi = 0.436$ (curve 1), $\Psi = 0.65$ (curve 2) and $\Psi = 0.685$ (curve 3).
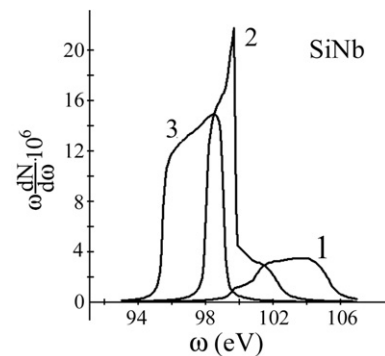

Fig. 4. The spectrum of collimated PXR from 100 keV electrons penetrating multilayer nanostructure. Presented curves have been calculated in the case $\Delta\Theta = \Delta\varphi = 0.07$, $T = 45$ Å, $a/T = 0.6$, $\Psi = 0.65$, $\langle\theta\rangle = 0.75$ (curve 1), $\langle\theta\rangle = 0.8$ (curve 2) and $\langle\theta\rangle = 0.85$ (curve 3).
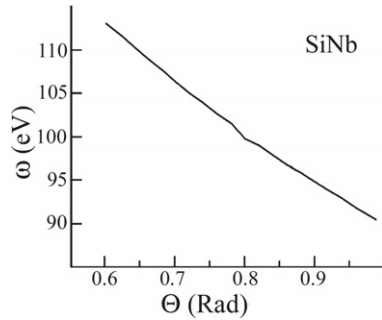
Fig. 5. The dependence $\omega^{PXR}(\theta)$ for PXR from 100 keV electrons penetrating multilayer nanostructure. Presented curve has been calculated in the case $\varphi = 0$, $T = 45$ Å, $a/T = 0.6$ and $\Psi = 0.65$.
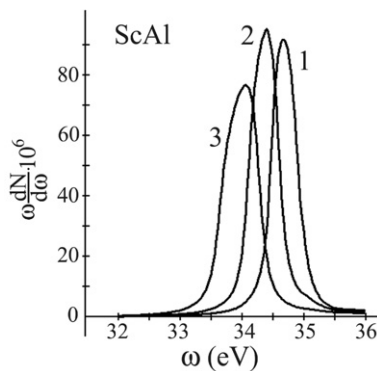

Fig. 6. The spectrum of collimated PXR from 100 keV electrons penetrating multilayer nanostructure. Presented curves have been calculated in the case $\Delta\Theta = \Delta\varphi = 0.07$, $T = 140$ Å, $a/T = 0.4$, $\Psi = 0.75$, $\langle\theta\rangle = 0.65$ (curve 1), $\langle\theta\rangle = 0.7$ (curve 2) and $\langle\theta\rangle = 0.75$ (curve 3).

The estimation of PXR intensity of the order of 10^{-6} photons/electron is the maximum possible value for given energy of emitting electrons. For example, PXR yield from 100 keV electrons penetrating Sc–Al nanostructure may run as high as approximately 10^{-5} photons/electron in accordance with the curves presented in Fig. 6.

4. Conclusions

Our analysis shows the possibility of creating a EUV source of quasi-monochromatic tunable photons based on PXR from non-relativistic electrons penetrating a multilayer nanostructure. The number of photons emitted to a photon collimator with angular size of the order of 0.07 rad is about 10^{-6}–10^{-5} per electron with energy of the order of 100 keV. The characteristic energy of photons emitted from the nanostructure with the period 10^{-6} cm is 100 eV. Spectral width of the emitted photon flux is a few eV.

Above estimations have been obtained on the basis of very simple formula for PXR spectral–angular distribution Eq. (22) derived under the assumption that the velocity of emitting electrons is small ($V \ll 1$). It is precisely this assumption that allowed us to neglect the contributions

of TR and DTR to the total emission yield. The contribution of terms omitted in the final formula for the emission spectral–angular distribution is about 20–30% for electron-energies of 100 keV.

The developed theory may be considered as preliminary only, since an influence of multiple scattering of emitting electrons on the emission characteristics has not been taken into account. This effect is most pronounced for the emission from non-relativistic electrons and will be considered in our further studies. The question of special interest for the problem of EUV source creation being discussed in the paper is the possibility to realize the PXR process in a multilayer nanostructure under conditions of the Cherenkov effect. Such conditions can be fulfilled easily for non-relativistic electrons in the frequency range tens eV because the dielectric susceptibility in the vicinity of photoabsorption edges of some elements has a value close to 1. Studies of EUV and X-ray emission from relativistic electrons in periodic media have shown the possibility to increase the PXR spectral–angular density under conditions being discussed [44]. The same follows from Eq. (22) for non-relativistic particles and, hence, PXR from non-relativistic electrons crossing a multilayer nanostructure under conditions of Cherenkov effect will be studied in our forthcoming paper.

Acknowledgements

References

[1] V.L. Ginzburg, I.M. Frank, J. Phys. (Moscow) 9 (1945) 3533.
[2] G. Garibian, Zh. Eksp. Teor. Fiz. 33 (1958) 1403 [Sov. Phys. JETP 6 (1958) 1079].
[3] M.L. Ter-Mikaelian, High Energy Electromagnetic Processes in Condensed Media, Wiley, New York, 1972.
[4] A.I. Alikhanian, F.R. Arutyunian, K.A. Ispirian, M.L. Ter-Mikaelian, Zh. Eksp. Teor. Fiz. 41 (1961) 2002 [Sov. Phys. JETP 14 (1962) 1471].
[5] M.L. Cherry, G. Hartman, D. Muller, T.A. Prince, Phys. Rev. D 10 (1974) 3594.
[6] M.A. Piestrup, D.G. Boyers, C.I. Pincus, J.L. Harris, H.S. Caplan, R.M. Silzer, D.M. Skopik, Appl. Phys. Lett. 59 (1991) 189.
[7] M.A. Piestrup, D.G. Boyers, C.I. Pincus, J.L. Harris, X.K. Maruyama, J.C. Bergstrom, H.S. Caplan, R.M. Silzer, D.M. Skopik, Phys. Rev. A 43 (1991) 3653.
[8] V.E. Pafomov, Proc. Lebedev Physical Institute RAS, 44, 25, 1971.
[9] G. Garibian, C. Yang, X-ray transition radiation, Ac. Sci. Arm. SSR, Yerevan, 1983.
[10] M.L. Cherry, D. Muller, T.A. Prince, Nucl. Instr. and Meth. 115 (1974) 141.
[11] Ya.B. Fainberg, N.A. Khizhniak, Zh. Eksp. Teor. Fiz. 32 (1957) 88 [Sov. Phys. JETP 5 (1957) 720].

[12] M.A. Piestrup, D.G. Boyers, C.I. Pincus, Q. Li, C.D. Hallewell, M.J. Moran, X.K. Maruyama, D.D. Snyder, R.M. Silzer, D.M. Skopik, G.B. Rothbart, Phys. Rev. A 45 (1992) 1183.

[13] N. Zhevago, in: Proceedings of the Second Symposium on Transition Radiation of High Energy Particles, Yerevan Physics Institute, Yerevan, Armenia, 1983, p. 200.

[14] C.T. Law, A.E. Kaplan, Opt. Lett. 12 (1987) 900.

[15] B. Pardo, J.-M. Andre, Phys. Rev. A 40 (1989) 1918.

[16] B. Pardo, J.-M. Andre, Phys. Rev. E 65 (2002) 036501.

[17] M.S. Dubovikov, Phys. Rev. A 50 (1994) 2008.

[18] B. Lastdrager, A. Tip, J. Verhoeven, Phys. Rev. E 61 (2000) 5767.

[19] N. Zhevago, V. Glebov, Phys. Lett. A 309 (2003) 311.

[20] I.D. Feranchuk, A. Ulyanenkov, Phys. Rev. B 63 (2001) 155318.

[21] V.G. Baryshevsky, I.D. Feranchuk, Zh. Eksp. Teor. Fiz. 61 (1971) 944 [Sov. Phys. JETP 34 (1972) 502].

[22] G.M. Garibian, S. Yang, Zh. Eksp. Teor. Fiz 61 (1971) 930 [Sov. Phys. JETP 34 (1972) 495].

[23] V.G. Baryshevsky, I.D. Feranchuk, J. Phys. (Paris) 44 (1983) 913.

[24] A. Caticha, Phys. Rev. A 40 (1989) 4322.

[25] Yu.N. Adishchev, S.A. Vorob'ev, B.N. Kalinin, S. Park, A.P. Potylitsyn, Zh. Eksp. Teor. Fiz. 90 (1986) 829 [Sov. Phys. JETP 63 (1986) 484].

[26] A.V. Shchagin, V.I. Pristupa, N.A. Khizhniak, Phys. Lett. A 148 (1990) 485.

[27] K.-H. Brenzinger, C. Herberg, B. Limburg, H. Backe, S. Dambach, H. Entenener, F. Hagenback, H. Hartmann, W. Schope, Th. Walcher, Z. Phys. A 358 (1997) 107.

[28] Yu.N. Adishchev, S. Arichev, A. Vnukov, et al., Nucl. Instr. and Meth. B 201 (2003) 114.

[29] Y.S. Korobochko, V.F. Kosmach, V.I. Mineev, Sov. Phys. JETP 21 (1965) 834.

[30] G.M. Reese, J.C.H. Spence, N. Yamamoto, Philos. Mag. A 49 (1984) 697.

[31] V.G. Baryshevsky, K.G. Batrakov, I.D. Feranchuk, A.A. Gurinovich, A.O. Grubich, A.S. Lobko, A.A. Rouba, B.A. Tarnovsky, P.F. Safronov, V.I. Stolyarsky, A.P. Ulyanenkov, LANL e-Print archive.

[32] I.D. Feranchuk, A. Ulyanenkov, J. Harada, J.C.H. Spence, Phys. Rev. E 62 (2000) 4225.

[33] I.D. Feranchuk, A.P. Ulyanenkov, Acta Cryst. A 57 (2001) 283.

[34] V.G. Baryshevsky, I.D. Feranchuk, A.P. Ulyanenkov, Parametric X-ray Radiation in Crystals Theory, Experiment and Applications, Springer, Berlin, 2005, 176p.

[35] N. Nasonov, V. Kaplin, S. Uglov, M. Piestrup, C. Gary, Phys. Rev. E 68 (2003) 036504.

[36] V. Kaplin, S. Uglov, V. Zabaev, M. Piestrup, C. Gary, N. Nasonov, M. Fuller, Appl. Phys. Lett. 76 (2000) 3647.

[37] N. Nasonov, V. Kaplin, S. Uglov, V. Zabaev, M. Piestrup, C. Gary, Nucl. Instr. and Meth. B 227 (2005) 41.

[38] A.E. Kaplan, S. Datta, Appl. Phys. Lett. 44 (1984) 661.

[39] S. Datta, A.E. Kaplan, Phys. Rev. A 31 (1985) 790.

[40] A.E. Kaplan, C.T. Law, P.L. Shkolnikov, Phys. Rev. E 82 (1995) 6795.

[41] M. Goldstein, S.H. Lee, Y.A. Shroff, P.J. Silverman, D. Williams, H. Park, M.A. Piestrup, R.H. Pantell, FEL applications in EUV Lithography, in: Proceedings of the 27th Free Electron Laser Conference, Stanford, CA, 2005, p. 422.

[42] B.W. Batterman, H. Cole, Rev. Mod. Phys. 36 (1964) 681.

[43] B. Henke, E. Gullikson, J. Davis, At. Data Nucl. Data Tables 54 (1993) 18.

[44] N. Nasonov, P. Zhukova, Phys. Lett. A 346 (2005) 367.